Catalysis Today xxx (xxxx) xxx–xxx

Contents lists available at ScienceDirect

Catalysis Today

journal homepage: www.elsevier.com/locate/cattod

Efficient oxidative dehydrogenation of ethanol by VO_x@MIL-101: On par with VO_x/ZrO_2 and much better than MIL-47(V)

Roman Bulánek*, Pavel Čičmanec, Jiří Kotera, Ishtvan Boldog*

University of Pardubice, Faculty of Chemical Technology, Department of Physical Chemistry, Studentská 573, CZ 532 10, Pardubice, Czech Republic

ARTICLE INFO

Keywords:
Oxidative dehydrogenation
Vanadium
Ethanol
Acetaldehyde
MIL-101
MOF

ABSTRACT

The possibility to apply metal organic framework (MOF) based catalysts for oxidation reaction in gas phase was explored. Catalytic activity of the vanadium oxide catalyst incorporated in MIL-101(Cr) as support was investigated in gas phase ethanol oxidative dehydrogenation (EtOH-ODH) and compared to that of MIL-47(V) metal organic framework material containing vanadium as central metal in the framework structure and to a classical VO_x/ZrO_2 supported vanadium oxide catalyst. It was found that vanadium species, incorporated in MIL-101(Cr) support by a variant of vapor deposition method, are stabilized in the form of well dispersed VO_x species (no vanadium pentoxide clusters was detected in the catalyst). The obtained VO_x@MIL-101(Cr) catalyst exhibited high selectivity towards acetaldehyde (up to 99%) at reaction temperatures not exceeding 200 °C. The catalytic activity of VO_x@MIL-101(Cr) catalyst reached an activity level comparable to that of the classical VO_x/ZrO_2 catalyst, but the specific productivity of acetaldehyde (3 kg_{AA} kg_{cat}^{-1} h^{-1}) was higher by 75% compared with productivity on VO_x/ZrO_2 due to much higher content of vanadium species, which could be hosted by the MOF. On the other hand, MIL-47(V) catalyst exhibited negligible activity seemingly due to coordinatively saturated character of the vanadium centers and/or too high stability of the V^{IV} oxidation state. This proof-of-concept study proved that application of MOF materials as host matrices for heterogeneous catalysts aiming oxidation reaction in gas phase could be efficient as demonstrated on the example of oxidative dehydrogenation of ethanol.

1. Introduction

Metal-organic frameworks (MOFs), also known as Porous Coordination Polymers (PCPs), are crystalline coordination compounds consisting of inorganic entities connected by means of organic bridging ligands [1]. They feature record holding surface areas, nearing the theoretical limits of porosity for any material at 10^4 m^2 g^{-1} [2], which creates significant prospects for their practical use [3–6]. Due to relatively low stability there are still no large scale uses of them, but opportunities for such industrial applications as small molecule storage [7–9], separation [10,11], heterogeneous catalysis [12–16], an recently also for electrical accumulator technologies [17,18] are significant.

There are two principal ways in incorporating the catalytic metal in the MOFs structure. The first one is the use of it as a part of the structure and the second is to load and subsequently immobilize the species in the pores of the matrix-material. Approximately a dozen of conventional vanadium-only based MOFs are known [19]. Among these only MIL-47(V) (MIL means Matérial Institut Lavoisier) with surface area up to 900 m^2 g^{-1} [20] and pore sizes up to 10.5 × 11 Å possesses sufficient chemical and thermal stability (up to 280 °C) to be a promising candidate for a multi-purpose catalyst. The higher stability of MIL-47(V) is explained by the fact that high temperature activation causes internal oxidation of V^{III} in the as-synthesized form to V^{IV}, which undergoes with minor structural reorganization [20]. The structure V^{IV} does not feature explicitly opened metal sites and the capacity towards easy charge flipping decreases due to increased structural stabilization. Some other MOFs like MIL-88(V) and MIL101(V) featuring V^{III} with opened metal sites would be much better candidates for catalytic materials, but unfortunately they convert at high temperatures to MIL-47(V) [21]. Vanadium based MOFs were demonstrated to have some catalytic effect [22] for such reaction as epoxidation of cyclohexene [23–25] and oxidative desulfurization [26] (however excesses of such agents as tertbuthylperoxide tend to degrade even the most robust MIL-47(V) or its derivatives [27]). MOFs based on mixed-metal clusters containing vanadium were occasionally synthesized, using chiefly aluminium-based prototypes, like $[Al(OH)L]_n$, where L= *p*-benzenedicarboxylate or *p*-naphtalenedicarboxylate [28] or MIL-53(Al) [29], which are essentially close to vanadium analogues, but testing of such

* Corresponding authors.
E-mail addresses: roman.bulanek@upce.cz (R. Bulánek), ishtvan.boldog@gmail.com (I. Boldog).

https://doi.org/10.1016/j.cattod.2018.07.034
Received 29 March 2018; Received in revised form 1 June 2018; Accepted 13 July 2018

materials in catalysis is still in its infancy. According to some researchers, until now there are practically no examples, where the metals incorporated in the clusters ('constitutional' metal ion) would express pronounced catalytic effect [30]. While this statement is disputable—the actual catalytic sites are associated with defects, which are inevitably generated at elevated temperatures even in coordinatively saturated MOFs like MIL-47(V) by disruption of some of the inherently labile coordination bonds—the approach targeting the use of the relatively non-numerous and not really modifiable SBUs as catalytic species has limited prospects. Somewhat broader possibilities exist, when the metal is incorporated in the organic linkers. Despite this group of compounds is still highly exotic due to additional synthetic steps necessary, examples of vanadium containing MOFs based on dipyridyl struts for oxidation of tetralin [31] or on salen-struts for asymmetric cyanosylilation do exists [32], even if the result are far from being breakthrough, due to the simplicity of the chosen reactions.

The second approach, namely the loading of the vanadium species in the pores of the MOFs provides much more opportunities regarding the choice of the catalytic species. The evident drawback is the decrease of the internal surface area and problems with different localization and non-uniform concentration of the species, and the material could be viewed rather as a heterogeneous catalytic mixture than an individual material. MOFs themselves are relatively labile compounds, while the ODH reaction conditions often demands temperatures over 200 °C as well as presence of oxygen and water as reaction products. MOFs with high hydrolytic stability are relatively rare, with main classes available being the carboxylate and azolate MOFs [33] (very recently the phosphonate class with appreciable porosities starts to emerge [34]). The azolate MOFs, with the exception of the more labile tetrazolates [35], possess inherently low oxidative stability, while among carboxylate MOFs one of the highest hydrolytic stability belongs to MIL-101(Cr) [36,37] due to kinetic inertness of the Cr^{3+} regarding ligand exchange [38]. The latter also possess very large pores, compared to an average MOF, excellent porosity (S_{BET} up to 4000 $m^2 g^{-1}$, ~29 Å largest accessible pore diameter as well as ~11 and 15 Å vdW (van der Waals dimensions) free pore opening in the pentagonal and hexagonal windows respectively [39–41]) and good thermal stability (up to 300–350 °C). Hence MIL-101 is a natural choice as a matrix material for general purpose catalysis. A special attention is drawn by encapsulated polyoxometallate species, POM@MIL-101 [42,43] (and refs. herein) particularly for oxidative catalysis, including vanadium containing [$Co(H_2O)_2(PW_9O_{34})_2$]@MIL-101 investigated for photocatalytic water oxidation [44], and $H_6[PMo_9V_3O_{40}]$@MIL-101(Cr)@SBA-15 for liquid phase benzene hydroxylation by oxygen gas at 80 °C [45]. Embedded catalysts of other types are less frequent, however the incorporation of metal-oxides in the receives growing attention [46]. There is only one report featuring catalytic vanadium containing materials of this type, the VO_x@MIL-101(Cr), demonstrated to catalyze high yield oxidations of sulfides to the respective sulfoxides/sulfones in polar media at room temperature [47].

A promising catalytic process employing vanadium species in MOFs is the oxidative dehydrogenation (ODH) of ethanol to acetaldehyde in the gas phase, which can be realized at temperatures as low as 200 °C. In addition, ethanol ODH can be also used as alternative process to the Wacker production of acetaldehyde from ethylene [48–50]. The benefit of using oxidative dehydrogenation is in possible implementation of the biomass-derived bio-ethanol, reduction of ethylene demand and improving the environmental friendliness by suppressing the production of toxic chlorinated by-products, typical for the Wacker process. Vanadium based catalysts belong to the most investigated and promising catalytic systems for the ODH of ethanol. Previous studies demonstrated that catalytic activity of the catalyst depends on nature of the support and speciation of vanadium complexes [50–54]. Regarding the activity and selectivity pair of parameters, the tetrahedral oligomeric vanadate species seem to be the most appropriate catalytic entities [50,52,55,56]. Nature of the support and its interaction with surface vanadyls play crucial role; VO_x/TiO_2 and VO_x/ZrO_2 catalysts exhibit significantly higher activity than vanadyls dispersed on silica and alumina supports [48,50,52,56]. To the best of our knowledge, no study on vanadium containing MOF catalysts for ODH of ethanol in gas phase was conducted. However, an obvious interest towards the related vanadium catalyzed ODH reaction of (cyclo)alkanes to respective (cyclo) alkenes as in the Ni-doped CoO_x@Nu-1000(Zr) [57] and $VO(acac)_2$@UiO-66(Zr) [58] functioning below 300 °C is emerging recently. These compounds feature well-defined anchoring of the catalytic species to the SBUs, which facilitates the interpretation of the catalytic test results. Unfortunately the Zr-based MOFs are not solvo-/hydrolytically stabile enough at elevated temperatures to be used for ODH of alcohols. In any case the elucidation of the anchoring mode and mechanism of catalysis of the encapsulated metal species in MOFs is of a great importance [59], and is topical for potential vanadium catalysts.

Proper, uniform deposition of the vanadium species in the pores of MOFs is an evident problem. In the case of metal oxide supports the high temperature 'annealing' (> 350 °C), which allows the vanadium species to redistribute uniformly on the surface makes the differences between deposition method not very pronounced. The widely used wet-impregnation method, which is particularly not uniform in general case, still ensures good results. MOFs are different from metal-oxide matrixes in regard of much lower thermal stabilities and low affinity of the organic moieties towards vanadium oxides, which is a hindrance for uniform distribution of the catalyst within a surface monolayer. Methods of low-temperature decomposition of species introduced by wet-impregnation without harsh calcination, i.e. 'burning' out the organic species, do exist, namely the decomposition of NH_4VO_3 (T_{decomp} > 180–220 °C [60], even if > 400 °C are typically used), which was successfully used for the deposition of vanadium species in the pores of MIL-101(Cr) [47]. However there is a dual-sided problem of vanadium loading optimization dealing with uniform distribution and low-processing temperatures in order to preserve maximally the MOF matrix.

Based on the above mentioned facts, we report here VO_x@MIL-101(Cr) catalytic system using a loading method related to vapor deposition with subsequent hydrolysis and activity testing of such catalyst in oxidative dehydrogenation of ethanol to acetaldehyde. Catalytic performance of the VO_x@MIL-101(Cr) material is compared to that of MIL-47(V) MOF, where vanadium is part of MOF structure, and VO_x/ZrO_2 catalysts, representing one of the most active and selective catalytic system among the classical metal-oxide supported materials.

2. Experimental part

2.1. Materials

2.1.1. Synthesis of MIL-47(V)

The material was synthesized using a slight modification of the original procedure [20,61]. 1.10 g (7.00 mmol) of VCl_3 and 1.16 g (7.00 mmol) of terephtalic acid were dissolved and thoroughly homogenized in 25.2 ml deionized water in a 50 ml Teflon lined autoclave. The sealed vessel was heated at 200 °C for three days. The solid product was filtered by gravity filtration through a filter paper. The dried product was transferred in an Erlenmeyer flask containing 40 ml of DMF and heated under slow stirring at 80 °C for 1 h. The solid was filtered out and washed with a small amount of DMF. The purification procedure, employing heating at 80 °C, was repeated once with DMF followed by one treatment with EtOH. After thorough final washing with EtOH the product was dried in air at 80 °C during 16 h. Yield of the yellow solid was 0.50 g (a few syntheses were worked up together and the given amounts of solvents and yield correspond to a single synthesis. Note also that even the relatively low temperature treatment in DMF was sufficient to oxidize the vanadium to V^{IV} state, so the obtained product is the conventional MIL-47(V) and not the MIL-47(V)-as precursor form).

2.1.2. Synthesis of MIL-101(Cr)

The material was synthesized using a modification of a fluoride-free method of preparation using nitric acid as an additive [62]. 2.00 g (5.00 mmol) of chromium(III) nitrate nonahydrate ($Cr(NO_3)_3{\cdot}9H_2O$) and 0.83 g of terephtalic acid (5.00 mmol) in a solution of 0.347 ml of concentrated nitric acid (60%) in 25 ml of deionized water were thoroughly homogenized in a 50 ml Teflon lined autoclave. The sealed vessel was heated for 8 h at 220 °C and cooled to room temperature ($-40\ °C\ h^{-1}$ gradient). The product was filtered by gravity filtration through a paper filter, washed thoroughly by multiple large portions of hot (~70-80 °C) deionized water. The same sequence of 2 × DMF and 1 × EtOH washings (30 ml in each case) as described in the synthesis of MIL-47(V) were applied (see above). The product, after final filtration and washing with a copious amount of EtOH was dried in air at 80 °C during 16 h yielding 904 mg of the product in a form a fine green powder (similarly to the previous compound, multiple syntheses were worked up together).

2.1.3. Synthesis of VO_x@MIL-101(Cr)

Before the loading, the MIL-101(Cr) material was degassed at 120 °C and 2 Torr in a Schlenk tube. The tube was cooled down and an excess of vanadium(V) oxytriisopropoxide ($VO(O\mathit{i}Pr)_3$) is added (approx. 4 ml of $VO(O\mathit{i}Pr)_3$ to 1 g of the MOF). The stirred slurry in 2 Torr vacuum was slowly heated up avoiding bumping until slow reflux started (~50–60 °C). The refluxing was continued for 2 h, followed by rising the temperature to 100 °C and slow distilling off the excess of $VO(O\mathit{i}Pr)_3$ (the vacuum during distillation was precisely in the range of 1–2 Torr; the $VO(O\mathit{i}Pr)_3$ recovered by distillation was reused for subsequent loadings). After fast removal of $VO(O\mathit{i}Pr)_3$ the formed powder was additionally left under the same temperature and pressure for 1 h and then cooled to r.t. The loaded sample was quickly transferred in air to a storage vial and hermetically sealed (1.95 g of $VO(O\mathit{i}Pr)_3$@MIL-101(Cr) in a form of a light green solid was isolated, which quickly turns yellow upon contact with moist air). Finally, the material loaded with vanadium species was controllably hydrolyzed by steaming in the flow of wetted nitrogen (flow rate 25 ml/min of gas containing 0.6 vol.% of water vapor) at 120 °C for 8 h.

2.2. Materials characterization

Chemical analysis was performed on the ICP-OES Optima 8000 Optical Emission Spectrometer (PerkinElmer) equipped with CCD detector. Meinhard and Scott-type mist chamber was used to measure the samples. Particles size and morphology of the synthesized materials was measured by scanning electron microscope JEOL JSM-7500 F with cold cathode-field emission at voltage of 5 kV in secondary electron imaging mode. Crystallinity of the samples was measured by D8-advance diffractometer (Bruker AXE, Germany) with Cu Kα radiation (λ = 1.5406 Å). The diffractometer was equipped by LynxEye detector, each diffractogram was measured with the step of 0.01° and integration time of 15 s per step. Specific surface area and porosity of the materials were estimated by N_2 adsorption/desorption isotherms measurement performed on ASAP 2020 volumetric apparatus (Micromeritics, USA). Prior to measurement, all samples were thoroughly degassed by slow heating (heating rate 0.5 °C/min) under turbomolecular pump vacuum up to 220 °C and degassed at target temperature for 12 h. Surface area was calculated according to both BET methodology for fixed 0.02 – 0.1 relative pressure (p/p_0) interval and Langmuir approach. Pore size distribution was calculated from adsorption branch by the nonlocal density functional theory approach by using the "N2@77 K" model for cylindrical pores and oxide surface (Microactive data reduction software, Micromeritics). Raman spectra were collected by Nicolet DXR2 Raman microscope (Thermo Scientific, USA) equipped by Smart excitation laser with wavelength of 785 nm. Spectra were recorded by accumulation of 180 scans (scan time was 20 s, resolution of $2\ cm^{-1}$, laser power was 2 mW).

2.3. Catalytic tests

Catalytic performances of the materials were measured by a Microactivity Effi microreactor (PID Eng&Tech, Spain). Catalyst weight used in tests was 25, 50 mg (and 75 mg for the VO_x/ZrO_2-10 sample) and total flow rate of reaction mixture was 6 l/h STP with the O_2/EtOH/He = 2.5/5/92.5 M ratio. Reaction was investigated at the temperature range 150–250 °C to avoid thermal decomposition of catalyst. The obtained products were monitored by on-line GC instrument (Agilent 7890B). Independent blank test with empty reactor proved negligible ethanol conversion (bellow 1%) under tested reaction conditions. Conversion of ethanol (X) and selectivity values (S_i) towards to the main reaction products were calculated according to Sachtler et al. [63] and supporting info (SI). For calculation of turn-over-frequency (TOF) and productivity (P) following equations have been utilized:

$$TOF = \frac{\dot{n}^0_{EtOH} X_{EtOH} M_V}{m_{cat} w_V} \quad (1)$$

$$P = \frac{\dot{n}^0_{EtOH} X_{EtOH} S_{AA} M_{AA}}{m_{cat}} \quad (2)$$

where $\dot{n}^0_{EtOH}$ denotes the inlet molar flow of ethanol, X_{EtOH} is the ethanol conversion (conversion degree equal to 15% was used), S_{AA} is the selectivity towards acetaldehyde, m_{cat} denotes the weight of catalyst (interpolated value for X_{EtOH} = 15% from plot X ~ m_{cat}), w_V is the mass fraction of vanadium, M_V is the atomic weight of vanadium (50.94 g mol^{-1}) and M_{AA} is the molar weight of acetaldehyde (44.05 g mol^{-1}).

Values of E_f factor for tested catalysts were calculated based on atomic balances from stoichiometric equations using all detected products in reaction mixture. The final expression using selectivity values S_i and molar masses of detected compounds was:

$$E_f = \frac{S_{C_2H_4}(M_{C_2H_4} + M_{H_2O}) + S_{(C_2H_5)_2O}\frac{M_{(C_2H_5)_2O} + M_{H_2O}}{2} + S_{AA}M_{H_2O}}{S_{AA}M_{AA}} \quad (3)$$

It must be noted that derived E_f represents theoretical value assuming nearly complete consumption of ethanol via its recycling and hence only products of the reaction are involved in the Eq. (3). Such definition was adopted to be comparable with E_f of the Wacker process operated also with 100% conversion of utilized ethene.

3. Results and discussion

3.1. Characterization of the catalysts

Content of vanadium in the as-prepared MOF catalysts was 20.1 wt.% and 12.5 wt.% for MIL-47(V) and VO_x@MIL-101(Cr), respectively. Chromium content in VO_x@MIL-101(Cr) catalyst was 9.3 wt.%. SEM micrographs of both MOFs are shown in Fig. 1. VO_x@MIL-101(Cr) material (Fig.1A) exhibits octahedral crystallites with average 300 nm long edge sizes, whereas MIL-47(V) catalyst has particles of cuboidal shape with the sizes in the range from 0.5 to several micrometer.

Fig. 2 shows the powder X-ray diffraction (PXRD) patterns of both types of MOF materials. The XRD pattern of the as-prepared MIL-101(Cr) agrees very well with theoretical simulated pattern (shown in the figure also). The diffraction pattern of the VO_x@MIL-101(Cr) catalyst is almost the same as that of the original MIL-101(Cr) support evidencing that introduction of the vanadium oxocomplexes into MIL-101(Cr) preserves the crystallinity of the matrix. The near perfect match also proves that there are no large crystallites outside of the pores are present (the possible nanocrystallites within the pores are not supposed to give appreciable diffraction signals due to different species and different possible localizations, which precludes long-range order). However, the XRD pattern of the VO_x@MIL-101(Cr) catalyst after catalytic test in ethanol ODH at 250 °C for 3 h reveals significant loss of

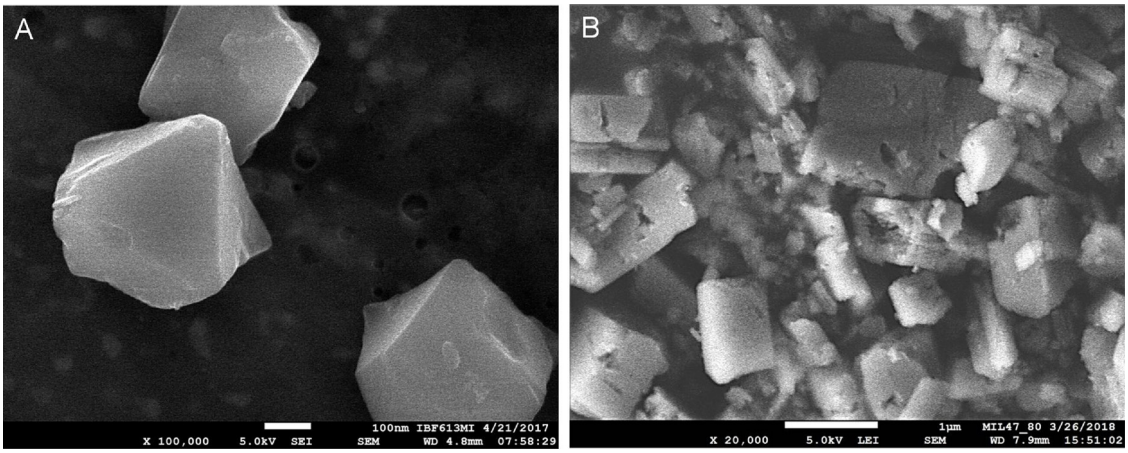

Fig. 1. SEM micrographs of VO_x@MIL-101(Cr) catalyst (A) and MIL-47(V) catalyst (B).

crystallinity, with only a fraction of long-range order retained (see pattern d in the left panel of the Fig. 2). The powder X-ray diffraction pattern (PXRD) of the as-synthesized MIL-47(V) exhibits intense and sharp diffraction peaks evidencing high quality of the crystals. Comparison with simulated patterns of MIL-47 with the presence of V^{III} and V^{IV} clearly shown that the position of the diffraction peaks in the obtained MIL-47(V) sample fit well with the simulated PXRD pattern of the conventional MIL-47(V^{IV}). It means that complete conversion of MIL-47(V^{III}), known as MIL-47(V)-as, to MIL-47(V^{IV}) took place during the low temperature treatment of the solid in dimethylformamide. In addition, it is noteworthy that the after-catalysis MIL-47(V) catalysts is deteriorated in much lesser extent compared to VO_x@MIL-101(Cr). It exhibits still sharp diffraction lines, slightly broader than as-synthesized one. There are a few weak broad additional peaks, which are localized quite close to the peaks of the MIL-47(V^{III}) form, which suggests that reduction of vanadium could take place (the slight differences in peak positions for these observed additional peaks and the peaks of the simulated MIL-47(V^{III}) could be explained by the fact that MIL-47(V) still possess some very minor flexibility, so characteristic to MIL-53(Al) analogue [64]).

The nitrogen adsorption/desorption isotherms of investigated materials and calculated pore size distribution curves are presented in Fig. 3 and textural parameters (*i.e.* BET and Langmuir surface areas and total pore volumes) are summarized in Table 1. The isotherm of as-synthesized MIL-101(Cr) sample has a shape close to type I isotherm exhibited by microporous materials and features a distinct sub-step around relative pressure 0.15 demonstrating presence of pores on the border between micro- and mesoporosity. It is also clearly seen from pore size distribution (PSD) curve of this sample (Fig. 3 curve a in right panel) exhibiting three distinct peak at 1.9, 2.1 and 2.8 nm. BET-specific surface area and total pore volume of the MIL-101(Cr) sample is 2439 $m^2\,g^{-1}$ and 1.21 $cm^3\,g^{-1}$ in good agreement with the textural data previously published in the literature for MIL-101(Cr) materials [40,62], (note, that the fluoride-free MIL-101(Cr) is characterized with slightly lower surface areas compared to the conventional synthesis, in which HF is used as additive). Introduction of the vanadium oxocomplexes significantly reduce surface area and pore volume of the material (by 50 rel.%) as is evident from adsorption isotherm of the VO_x@MIL-101(Cr) sample (Fig. 3b). Interestingly, presence of the guest vanadium species influences pore volumes unequally; pores at 2.1 nm almost complete disappeared, whereas the largest pores became narrower (PSD peak shifted from 2.8 to 2.6 nm) and their volume decreased. On the other hand, the smallest pores (with diameter 1.9 nm) were virtually unaffected by the presence of VO_x species. VO_x@MIL-101(Cr) sample after catalytic tests conducted up to 250 °C exhibits low porosity with surface area of only 138 $m^2\,g^{-1}$ and total pore volume 0.08 $cm^3\,g^{-1}$. The latter observation indicates that in current form the catalyst is not stabile for prolonged use at 250 °C, which is consistent with the drop of selectivity and productivity at temperatures over 200 °C. It might happen due to redistribution/leaching of vanadium

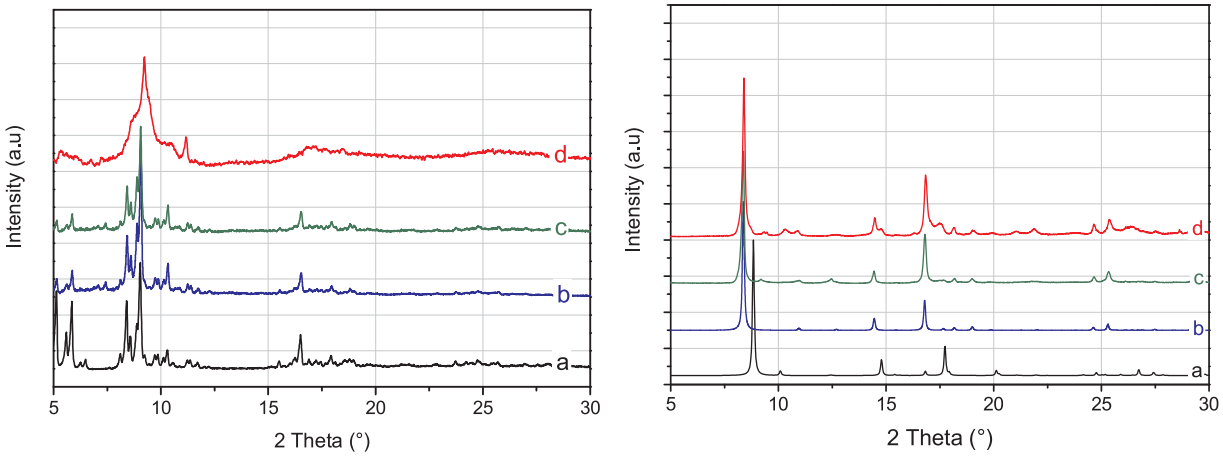

Fig. 2. PXRD patterns of the investigated MOFs. Left panel: a – simulated pattern of the MIL-101(Cr), followed by the experimental patterns of b – MIL-101(Cr), c – VO_x@MIL-101(Cr), d - VO_x@MIL-101(Cr) after ethanol ODH reaction at 250 °C for 3 h. Right panel: a – simulated pattern of the MIL-47(V^{III}) material known as 'MIL-47(V)-as' [20], b - simulated pattern of the MIL-47(V^{IV}) material, followed by the experimental patterns of the MIL-47(V) catalyst and d - MIL-47(V) catalyst after ethanol ODH reaction at 250 °C for 3 h.

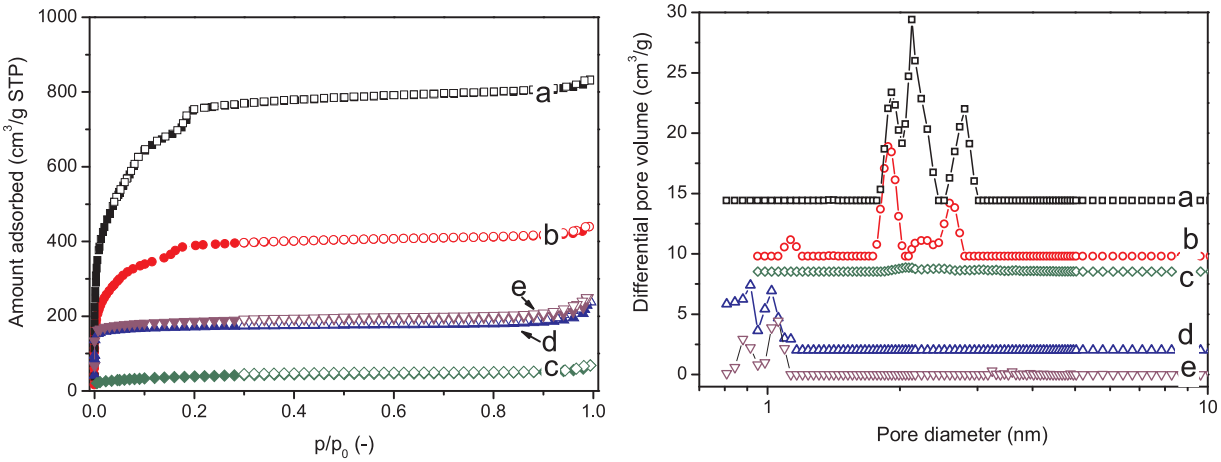

Fig. 3. N_2 adsorption/desorption isotherms of the investigated samples (left panel) and pore size distribution curves calculated by NLDFT methodology (right panel). a – MIL-101(Cr), b – VO_x@MIL-101(Cr), c - VO_x@MIL-101(Cr)-r, d – MIL-47(V), e - MIL-47(V)-r (the suffix '–r' stands for 'after catalytic tests, i.e. reactions').

Table 1
Textural properties of the catalysts.

	c_V wt.%	S_{BET} $m^2\,g^{-1}$	S_{Lang} $m^2\,g^{-1}$	V_p $cm^3\,g^{-1}$
MIL-101(Cr)	–	2439	2720	1.21
VOx@MIL-101(Cr)	12.5	1258	1530	0.61
VOx@MIL-101(Cr)-r[a]	12.4	138	221	0.08
MIL-47(V)	20.1	681	762	0.30
MIL-47(V)-r[a]	20.1	730	856	0.33

[a] r denotes sample after reaction test.

species obturating the pores. Adsorption isotherms recorded on MIL-47(V) samples resemble type I shape of the isotherm according to IUPAC nomenclature typical for ultra-microporous solids (Fig. 3, line d and e). As-prepared MIL-47(V) sample exhibits BET-specific surface area of 681 $m^2\,g^{-1}$ and total pore volume 0.30 $cm^3\,g^{-1}$. Sample after reaction exhibits slightly larger BET-specific surface area (730 $m^2\,g^{-1}$) and pore volume (0.33 $cm^3\,g^{-1}$). The increase of the surface area is associated with complete removal of the residual adsorbed terephtalic acid from the pores during the catalytic tests.

The Raman spectra (Fig. 4) provide additional information about the structure and the state of vanadium species in the composite materials. All Raman spectra exhibit intense bands at 1615 and ca. 1450 cm^{-1} ascribed to asymmetric and symmetric −COO stretching

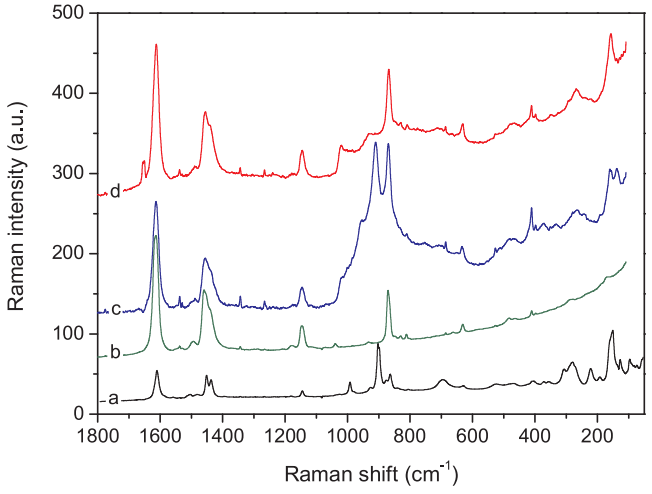

Fig. 4. Raman spectra of the synthesized samples. a – MIL-47(V), b - MIL-101(Cr), c - VO(O*i*Pr)$_n$@MIL-101(Cr), d - VO_x@MIL-101(Cr).

vibrations of the terephtalate linkers and band at 867 cm^{-1} assigned usually to the benzene ring−COO group bending vibration mode [65,66]. Besides these characteristic bands of terephtalate linker, the spectra also exhibit bands related to presence of vanadium. Intense band at 902 cm^{-1} observed in the Raman spectrum of the MIL-47(V) is caused by $V^{IV}=O$ group's stretching vibration [67]. The Raman spectrum of the intermediary VO(O*i*Pr)$_3$@MIL-101(Cr) exhibits intense band at 910 cm^{-1} accompanied by a few poorly distinguished bands in 1030-920 cm^{-1} region originating from the triisopropoxide moieties (most likely caused by $O=V(-O-)_n$ vibration [68]. The Raman spectrum of the VO_x@MIL-101(Cr) sample after hydrolysis reveals that typical Raman bands of the MIL-101(Cr) support are preserved while the spectral features of the triisopropoxide moiety disappeared and new bands located at 1021 and 934 cm^{-1}, which are assigned to terminal V=O and bridging V−O−V vibrations [69] respectively, showed up in the spectrum. This observation proves that the structure of the MIL-101(Cr) matrix is not damaged and complete hydrolysis of the isopropoxides took place. Vanadium species are incorporated in the pores of the MIL-101(Cr) in the form of dispersed vanadate species, no bulk vanadium pentoxide clusters are present as proven by absence of its characteristic band at 995 cm^{-1}.

3.2. Catalytic tests

Vanadium species anchored on the surface of MIL-101(Cr) support catalyzes the oxidative dehydrogenation at temperature as low as 175 °C. The effect of reaction temperature on conversion of reactant and product selectivity is reported in the Fig. 5A. According to the data, at temperatures up to 200 °C the reaction produces almost exclusively acetaldehyde (more than 98% of selectivity) with traces of diethylether. At higher reaction temperature, reactant conversion steeply increases and other products, like ethene and carbon dioxide, occur with aggregate selectivity not exceeding 15% at the highest temperature (250 °C). At this temperature, oxygen is almost completely consumed and ethanol conversion reaches 78%. It is important to note that conversion of ethanol at 250 °C is changing in time-on-stream, which is attributed to the partial collapse of the MOF framework as documented by PXRD and N_2 adsorption isotherm measurements (see Figs. 2 and 3). However, sample deactivation was not observed at 200 °C, as is illustrated in the Fig. 5B, where ethanol conversion and product selectivity is shown as a function of time on stream at 200 °C. It means that VO_x@MIL-101(Cr) catalyst is able to activate ethanol at temperature as low as 200 °C and convert it to acetaldehyde with reasonable high rate and excellent selectivity. On the other hand, despite high concentration of vanadium in MIL-47(V) MOF, its catalytic activity was negligible. Conversion of ethanol over 25 mg of sample did not exceed 2% even at

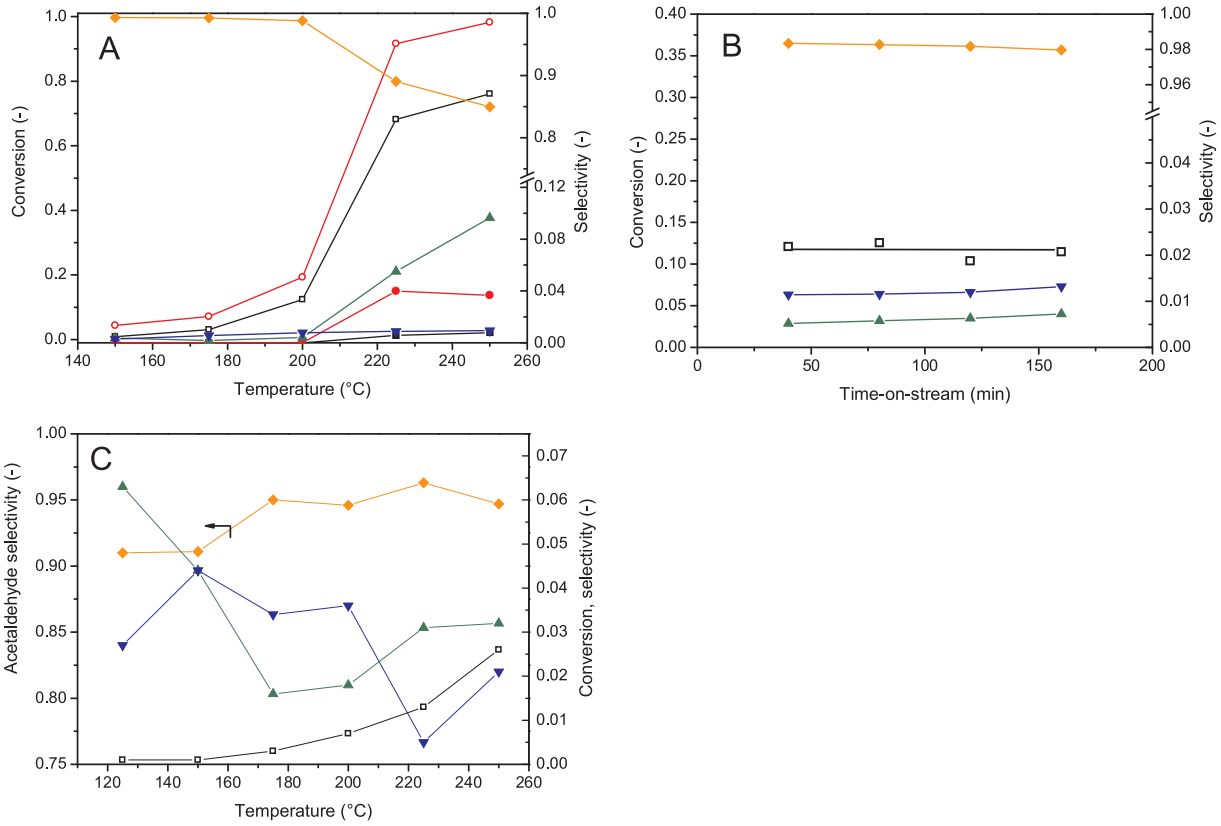

Fig. 5. Catalytic performance of the 25 mg MOF catalysts in ethanol ODH. (A) Conversion of the reactant (open symbols, square – ethanol, circle - oxygen) and selectivity toward individual products (full symbols, diamond – acetaldehyde, circle $-CO_2$, up triangle – ethene, down triangle – diethylether, square $-CO$) over VO_x@MIL-101(Cr) as a function of the reaction temperature. (B) Ethanol conversion and product selectivities as function of the time-on-stream at 200 °C over VO_x@MIL-101(Cr). (C) Conversion of the reactant and selectivity toward individual products over MIL-47 as a function of the reaction temperature.

250 °C. The reason for such low activity is most probably the inaccessibility of active centers and/or too high stability of the V^{IV} oxidation state. Selectivity to acetaldehyde was also slightly lower compared to VO_x@MIL-101(Cr) catalyst (no higher than 96%) and ethylene was produced with selectivity around 4%, probably due to presence of acidic V—OH sites on the MIL-47(V) surface [66]. Selectivity to ethene start to grow at temperature above 200 °C, but the values did not exceed 8%. Gobara et al. reported significant activity of MIL-101(Cr) catalyst in dehydration of ethanol to ethene with 26% yield at 300 °C and improved yields in the case of M@MIL-101(Cr) composites (where M = Ni, Pt) [70].

For proper evaluation of functioning of the VO_x@MIL-101(Cr) catalyst, it is worth to compare it with well-known benchmarks. However, direct comparison of performances of various catalytic systems is not straightforward due to application of different reaction conditions, which have strong effect on the overall performance. Thus, we are going to compare and discuss the catalytic performance of the VO_x@MIL-101(Cr) primarily with the VO_x/ZrO_2 catalytic system, which exhibited very good performance at the 200 °C, investigated in our group recently under precisely the same conditions. Comparative results of catalytic tests in ODH of ethanol at 200 °C together with corresponding catalytic data for the best performing VO_x/ZrO_2-5 and VO_x/ZrO_2-10 catalyst references of similar vanadium concentration, which were reported in our recent article [71], are summarized in Table 2. All reported data corresponds to the same conversion degree 15% obtained by varying the weight of the catalyst samples in the reactor.

The main reaction product formed over the VO_x@MIL-101(Cr) at 200 °C was acetaldehyde, while minor amounts of ethene and diethylether were also formed, but no carbon oxides or acetic acid formation were detected. The composition of the products formed over VO_x/ZrO_2 catalysts under the same conditions is very close.

Table 2
Results of catalytic tests at 200 °C compared at iso-conversion degree X_{iso} = 15%.

	Selectivity			TOF[b]	P[c]	E_f[d]
	C_2H_4 %	$(C_2H_5)_2O$ %	CH_3CHO %	h^{-1}	$kg_{AA}/kg_{cat}/h$	kg/kg_{AA}
VO_x/ZrO_2-5[a]	0.3	1.2	98.5	55	1.7	0.425
VO_x/ZrO_2-10[a]	0.5	2.5	97.0	22	1.2	0.441
VOx@MIL-101 (Cr)	0.6	1.1	98.3	29	3.0	0.427

[a] the detailed characterization and catalytic performance is described in Ref. [71].
[b] the calculated specific activity is based on Eq. (1).
[c] the calculated productivity is based on Eq. (2).
[d] the E-factor value is calculated on the basis of Eq. (3).

The specific activity of vanadium oxide species in the VO_x@MIL-101(Cr) catalyst expressed by the TOF value is roughly half in comparison to best performing zirconia supported VO_x catalyst VO_x/ZrO_2-5. Nevertheless this material was close to its optimal vanadium concentration and further increase of vanadia content led to decrease of activity for this type of material due to formation of more polymerized bulk V_2O_5-like species [71] as it can be demonstrated on the example of VO_x/ZrO_2-10 catalyst which has even lower value of TOF (or more precisely value of the specific activity) than the MIL-101 supported VO_x catalyst in this contribution. It can note that similar or slightly higher activity can be expected for VO_x/TiO_2 systems, while VO_x/SiO_2 and VO_x/Al_2O_3 usually exhibit significantly lower activity (5-20-times) [72].

The productivity of catalyst P (in kg of product per kg of catalyst and time unit) belongs to most frequently used characteristics for the comparison of the applicability of the catalysts in industry. The values of calculated productivity for our set of catalysts clearly indicate that the productivity of the VO_x@MIL-101(Cr) catalyst is at value ca. 3 kg_{AA} kg_{cat}^{-1} h^{-1} and higher than productivity of both zirconia supported samples due to its significantly higher content of VO_x catalytic species. Furthermore, the calculated VO_x surface density for our MIL-101 supported sample is *ca.* 0.65 V atoms per nm^2 area and this is below theirs monolayer capacity for the most supporting materials (but it must be stressed that monolayer capacity for MOFs makes not much physical sense, because the organic linkers, associated with a large part of the surface area, only weakly interact with vanadium oxides and could not be viewed as a proper support) [50,52,54]. Therefore we believe there is still a room for the improvement of the productivity of this type of catalysts.

The selectivity of catalytic process towards desired product is practically a more important factor than the activity of catalyst. All tested catalysts exhibit very high selectivity to acetaldehyde higher than 98% for both VO_x@MIL-101(Cr) and VO_x/ZrO_2-5. Both observed by-products formed in the reaction are yielded by parallel reactions catalyzed concurrently on acid sites as already documented for VO_x/ZrO_2-10 [71]. The impact of the formation of unwanted compounds in the reaction is another classification criterion, which should be considered during the catalysts or catalytic processes evaluation. The so called E-factor, representing the "*weight of waste formed per one kilogram of desired product produced*", is frequently used for the characterization and evaluation of this aspect of catalytic processes. The values of E-factor calculated for tested set of catalysts using Eq. 3 are presented in the Table 2. The theoretical lower limit of the E-factor for the ethanol oxidative dehydrogenation assuming 100% selectivity towards acetaldehyde is M_{H_2O}/M_{AA} = 0.409 kg of waste per kg of acetaldehyde for a stoichiometric reaction. All tested catalysts deviate only in the order of few percent from this theoretical limit due to their high selectivity discussed in the paragraph above. VO_x@MIL-101(Cr) catalyst has the value of the E-factor approximately the same as the VO_x/ZrO_2-5 catalysts, but in the same time demonstrating approx. 75% higher productivity. It must be noted that simple comparison of the E-factor values for completely different processes can be misleading. According to [73], the E-factor for a two stage Wacker process is approximately 0.07 kg of waste per kg of acetaldehyde, nevertheless at least 60% of this waste is represented by chlorinated aldehydes and alkanes. From this point of view water (more than 95%), ethene and diethylether produced in the oxidative dehydrogenation of ethanol offer a much cleaner process.

4. Conclusions

In summary, a proof-of-concept study of a MIL-101(Cr) matrix hosting VO_x species, inspired by high surface area, volume- and sizes of the pores as well as distinct stability of the host among other MOF material peers, was conducted. VO_x@MIL-101(Cr) catalyst represents promising and interesting catalytic system for ethanol conversion to value-added acetaldehyde and is able to compete with vanadium catalysts deposited on traditional inorganic supports. At 200 °C, VO_x@MIL-101(Cr) exhibited noteworthy catalytic activity and very high selectivity to the desired acetaldehyde resulting in 3 kg_{AA} kg_{cat}^{-1} h^{-1} productivity, which is 75% higher compared to VO_x/ZrO_2. Raman spectra revealed that inner surface of the structural pores of the MIL-101(Cr) MOF is suitable for anchoring and stabilization of the vanadyl species. Contrary to VO_x@MIL-101(Cr), MIL-47(V) metal organic framework material, having 'constitutional' vanadium ions in the structure, exhibited very poor catalytic activity, which might reflect generally low prospects for precisely this type of materials. Most probably the low activity is associated with inaccessibility of active (vanadium) centers and/or too high stability of the V^{IV} oxidation state. The observed high activity of VO_x@MIL-101(Cr) is very interesting as the absolute majority of vanadium catalysts used for similar reactions are strongly bound by a metal-oxide support, while the involvement of the latter is viewed as crucial for activation, rationalized *e.g.* through its involvement in the Mars-van Krevelen mechanism. The anchorage of VO_x species to the MOF support is much weaker and should be sustained by coordination bonding with the chromium oxo/hydroxy carboxylate clusters. It was suggested before that individual VO_x species, though completely impractical due to considerable solubility in water, might be as effective catalysts as their metal-oxide supported forms. The presented case opens up an interesting opportunity for investigation of quasi-isolated VO_x species in relatively neutral matrices, their mode of anchorage and alternative immobilization methods in a range of modified forms.

Acknowledgements

A financial support of the Czech Science Foundation under the project Center of Excellence No. 106/12/G015 and grant LM2015082 Center of Materials and Nanotechnologies from the Ministry of Education, Youth and Sports of the Czech Republic is highly acknowledged.

References

[1] B. Li, H.-M. Wen, Y. Cui, W. Zhou, G. Qian, B. Chen, Emerging multifunctional metal-organic framework materials, Adv. Mater. 28 (2016) 8819–8860, https://doi.org/10.1002/adma.201601133.
[2] O.K. Farha, I. Eryazici, N.C. Jeong, B.G. Hauser, C.E. Wilmer, A.A. Sarjeant, R.Q. Snurr, S.T. Nguyen, A.Ö. Yazaydın, J.T. Hupp, Metal–organic framework materials with ultrahigh surface areas: is the sky the limit? J. Am. Chem. Soc. 134 (2012) 15016–15021, https://doi.org/10.1021/ja3055639.
[3] P. Silva, S.M.F. Vilela, J.P.C. Tomé, F.A. Almeida Paz, Multifunctional metal–organic frameworks: from academia to industrial applications, Chem. Soc. Rev. 44 (2015) 6774–6803, https://doi.org/10.1039/C5CS00307E.
[4] X.-Y. Yang, L.-H. Chen, Y. Li, J.C. Rooke, C. Sanchez, B.-L. Su, Hierarchically porous materials: synthesis strategies and structure design, Chem. Soc. Rev. 46 (2017) 481–558, https://doi.org/10.1039/C6CS00829A.
[5] B. Li, M. Chrzanowski, Y. Zhang, S. Ma, Applications of metal-organic frameworks featuring multi-functional sites, Coord. Chem. Rev. 307 (2016) 106–129, https://doi.org/10.1016/j.ccr.2015.05.005.
[6] Y. Cui, B. Li, H. He, W. Zhou, B. Chen, G. Qian, Metal–organic frameworks as platforms for functional materials, Acc. Chem. Res. 49 (2016) 483–493, https://doi.org/10.1021/acs.accounts.5b00530.
[7] W. Lu, D. Yuan, T.A. Makal, Z. Wei, J.-R. Li, H.-C. Zhou, Highly porous metal-organic framework sustained with 12-connected nanoscopic octahedra, Dalton Trans. 42 (2013) 1708–1714, https://doi.org/10.1039/c2dt32479b.
[8] B. Li, H.-M. Wen, W. Zhou, B. Chen, Porous metal–organic frameworks for gas storage and separation: what, how, and why? J. Phys. Chem. Lett. 5 (2014) 3468–3479, https://doi.org/10.1021/jz501586e.
[9] J. Sculley, D. Yuan, H.-C. Zhou, The current status of hydrogen storage in metal–organic frameworks—updated, Energy Environ. Sci. 4 (2011) 2721, https://doi.org/10.1039/c1ee01240a.
[10] Y. Wang, D. Zhao, Beyond equilibrium: metal–organic frameworks for molecular sieving and kinetic gas separation, Cryst. Growth Des. 17 (2017) 2291–2308, https://doi.org/10.1021/acs.cgd.7b00287.
[11] J.-R. Li, R.J. Kuppler, H.-C. Zhou, Selective gas adsorption and separation in metal-organic frameworks, Chem. Soc. Rev. 38 (2009) 1477–1504, https://doi.org/10.1039/b802426j.
[12] Y.-B. Huang, J. Liang, X.-S. Wang, R. Cao, Multifunctional metal–organic framework catalysts: synergistic catalysis and tandem reactions, Chem. Soc. Rev. 46 (2017) 126–157, https://doi.org/10.1039/C6CS00250A.
[13] J. Liu, L. Chen, H. Cui, J. Zhang, L. Zhang, C.-Y. Su, Applications of metal–organic frameworks in heterogeneous supramolecular catalysis, Chem. Soc. Rev. 43 (2014) 6011–6061, https://doi.org/10.1039/C4CS00094C.
[14] T. Zhang, W. Lin, Metal–organic frameworks for artificial photosynthesis and photocatalysis, Chem. Soc. Rev. 43 (2014) 5982–5993, https://doi.org/10.1039/C4CS00103F.
[15] A. Dhakshinamoorthy, M. Alvaro, H. Garcia, Commercial metal–organic frameworks as heterogeneous catalysts, Chem. Commun. (Camb.) 48 (2012) 11275, https://doi.org/10.1039/c2cc34329k.
[16] J. Lee, O.K. Farha, J. Roberts, K. a Scheidt, S.T. Nguyen, J.T. Hupp, Metal-organic framework materials as catalysts, Chem. Soc. Rev. 38 (2009) 1450–1459, https://doi.org/10.1039/b807080f.
[17] X. Cao, C. Tan, M. Sindoro, H. Zhang, Hybrid micro-/nano-structures derived from metal–organic frameworks: preparation and applications in energy storage and conversion, Chem. Soc. Rev. 46 (2017) 2660–2677, https://doi.org/10.1039/C6CS00426A.

[18] H. Wang, Q.-L. Zhu, R. Zou, Q. Xu, Metal-organic frameworks for energy applications, Chem 2 (2017) 52–80, https://doi.org/10.1016/j.chempr.2016.12.002.

[19] P. der Voort, K. Leus, Y.-Y. Liu, M. Vandichel, V. Van Speybroeck, M. Waroquier, S. Biswas, Vanadium metal-organic frameworks: structures and applications, New J. Chem. 38 (2014) 1853–1867, https://doi.org/10.1039/c3nj01130e.

[20] K. Barthelet, J. Marrot, D. Riou, G. Férey, A breathing hybrid organic–inorganic solid with very large pores and high magnetic characteristics, Angew. Chemie Int. Ed. 41 (2002) 281, https://doi.org/10.1002/1521-3773(20020118)41:2<281::AID-ANIE281>3.0.CO;2-Y.

[21] F. Carson, J. Su, A.E. Platero-Prats, W. Wan, Y. Yun, L. Samain, X. Zou, Framework isomerism in vanadium metal-organic frameworks: MIL-88B(V) and MIL-101(V), Cryst. Growth Des. 13 (2013) 5036–5044, https://doi.org/10.1021/cg4012058.

[22] M. Vandichel, S. Biswas, K. Leus, J. Paier, J. Sauer, T. Verstraelen, P. der Voort, M. Waroquier, V. Van Speybroeck, Catalytic performance of vanadium MIL-47 and linker-substituted variants in the oxidation of cyclohexene: a combined theoretical and experimental approach, Chempluschem 79 (2014) 1183–1197, https://doi.org/10.1002/cplu.201402007.

[23] K. Leus, I. Muylaert, M. Vandichel, G.B. Marin, M. Waroquier, V. Van Speybroeck, P. Van Der Voort, The remarkable catalytic activity of the saturated metal organic framework V-MIL-47 in the cyclohexene oxidation, Chem. Commun. (Camb.) 46 (2010) 5085, https://doi.org/10.1039/c0cc01506g.

[24] K. Leus, M. Vandichel, Y.-Y. Liu, I. Muylaert, J. Musschoot, S. Pyl, H. Vrielinck, F. Callens, G.B. Marin, C. Detavernier, P.V. Wiper, Y.Z. Khimyak, M. Waroquier, V. Van Speybroeck, P. Van Der, Voort, The coordinatively saturated vanadium MIL-47 as a low leaching heterogeneous catalyst in the oxidation of cyclohexene, J. Catal. 285 (2012) 196–207, https://doi.org/10.1016/j.jcat.2011.09.014.

[25] Y.-Y. Liu, K. Leus, M. Grzywa, D. Weinberger, K. Strubbe, H. Vrielinck, R. Van Deun, D. Volkmer, V. Van Speybroeck, P. Van Der Voort, Synthesis, structural characterization, and catalytic performance of a vanadium-based metal-organic framework (COMOC-3), Eur. J. Inorg. Chem. (2012) 2819–2827, https://doi.org/10.1002/ejic.201101099 2012.

[26] N.D. McNamara, G.T. Neumann, E.T. Masko, J.A. Urban, J.C. Hicks, Catalytic performance and stability of (V) MIL-47 and (Ti) MIL-125 in the oxidative desulfurization of heterocyclic aromatic sulfur compounds, J. Catal. 305 (2013) 217–226, https://doi.org/10.1016/j.jcat.2013.05.021.

[27] K. Leus, G. Vanhaelewyn, T. Bogaerts, Y.Y. Liu, D. Esquivel, F. Callens, G.B. Marin, V. Van Speybroeck, H. Vrielinck, P. Van Der Voort, Ti-functionalized NH2-MIL-47: an effective and stable epoxidation catalyst, Catal. Today 208 (2013) 97–105, https://doi.org/10.1016/j.cattod.2012.09.037.

[28] O. Kozachuk, M. Meilikhov, K. Yusenko, A. Schneemann, B. Jee, A.V. Kuttatheyil, M. Bertmer, C. Sternemann, A. Pöppl, R.A. Fischer, A solid-solution approach to mixed-metal metal-organic frameworks - detailed characterization of local structures, defects and breathing behaviour of Al/V frameworks, Eur. J. Inorg. Chem. (2013) 4546–4557, https://doi.org/10.1002/ejic.201300591 2013.

[29] I. Nevjestić, H. Depauw, K. Leus, G. Rampelberg, C.A. Murray, C. Detavernier, P. Van Der Voort, F. Callens, H. Vrielinck, In situ electron paramagnetic resonance and X-ray diffraction monitoring of temperature-induced breathing and related structural transformations in activated V-Doped MIL-53(Al), J. Phys. Chem. C. 120 (2016) 17400–17407, https://doi.org/10.1021/acs.jpcc.6b04402.

[30] A. Dhakshinamoorthy, A.M. Asiri, H. Garcia, Metal-organic frameworks as catalysts for oxidation reactions, Chem. –A Eur. J. 22 (2016) 8012–8024, https://doi.org/10.1002/chem.201505141.

[31] H.G.T. Nguyen, M.H. Weston, A.A. Sarjeant, D.M. Gardner, Z. An, R. Carmieli, M.R. Wasielewski, O.K. Farha, J.T. Hupp, S.T. Nguyen, Design, synthesis, characterization, and catalytic properties of a large-pore metal-organic framework possessing single-site Vanadyl(monocatecholate) Moieties, Cryst. Growth Des. 13 (2013) 3528–3534, https://doi.org/10.1021/cg400500t.

[32] A. Bhunia, S. Dey, J.M. Moreno, U. Diaz, P. Concepcion, K. Van Hecke, C. Janiak, P. Van Der Voort, A homochiral vanadium–salen based cadmium bpdc MOF with permanent porosity as an asymmetric catalyst in solvent-free cyanosilylation, Chem. Commun. (Camb.) 52 (2016) 1401–1404, https://doi.org/10.1039/C5CC09459C.

[33] C. Wang, X. Liu, N. Keser Demir, J.P. Chen, K. Li, Applications of water stable metal–organic frameworks, Chem. Soc. Rev. 45 (2016) 5107–5134, https://doi.org/10.1039/C6CS00362A.

[34] T. Zheng, Z. Yang, D. Gui, Z. Liu, X. Wang, X. Dai, S. Liu, L. Zhang, Y. Gao, L. Chen, D. Sheng, Y. Wang, J. Diwu, J. Wang, R. Zhou, Z. Chai, T.E. Albrecht-Schmitt, S. Wang, Overcoming the crystallization and designability issues in the ultrastable zirconium phosphonate framework system, Nat. Commun. 8 (2017) 15369, https://doi.org/10.1038/ncomms15369.

[35] V. Colombo, S. Galli, H.J. Choi, G.D. Han, A. Maspero, G. Palmisano, N. Masciocchi, J.R. Long, High thermal and chemical stability in pyrazolate-bridged metal–organic frameworks with exposed metal sites, Chem. Sci. 2 (2011) 1311, https://doi.org/10.1039/c1sc00136a.

[36] J.J. Low, A.I. Benin, P. Jakubczak, J.F. Abrahamian, S.A. Faheem, R.R. Willis, Virtual high throughput screening confirmed experimentally: porous coordination polymer hydration, J. Am. Chem. Soc. 131 (2009) 15834–15842, https://doi.org/10.1021/ja9061344.

[37] A.J. Howarth, Y. Liu, P. Li, Z. Li, T.C. Wang, J.T. Hupp, O.K. Farha, Chemical, thermal and mechanical stabilities of metal–organic frameworks, Nat. Rev. Mater. 1 (2016) 15018, https://doi.org/10.1038/natrevmats.2015.18.

[38] N.C. Burtch, H. Jasuja, K.S. Walton, Water Stability and adsorption in metal–organic frameworks, Chem. Rev. 114 (2014) 10575–10612, https://doi.org/10.1021/cr5002589.

[39] G. Férey, C. Serre, C. Mellot-Draznieks, F. Millange, S. Surblé, J. Dutour, I. Margiolaki, A hybrid solid with giant pores prepared by a combination of targeted chemistry, simulation, and powder diffraction, Angew. Chem. Int. Ed. Engl. 43 (2004) 6296–6301, https://doi.org/10.1002/anie.200460592.

[40] D.-Y. Hong, Y.K. Hwang, C. Serre, G. Férey, J.-S. Chang, Porous chromium terephthalate MIL-101 with coordinatively unsaturated sites: surface functionalization, encapsulation, sorption and catalysis, Adv. Funct. Mater. 19 (2009) 1537–1552, https://doi.org/10.1002/adfm.200801130.

[41] G. Férey, C. Mellot-Draznieks, C. Serre, F. Millange, J. Dutour, S. Surblé, I. Margiolaki, A chromium terephthalate-based solid with unusually large pore volumes and surface area, Science (80-) 80 (309) (2005) 2040–2042, https://doi.org/10.1126/science.1116275.

[42] D.-Y. Du, J.-S. Qin, S.-L. Li, Z.-M. Su, Y.-Q. Lan, Recent advances in porous polyoxometalate-based metal–organic framework materials, Chem. Soc. Rev. 43 (2014) 4615–4632, https://doi.org/10.1039/C3CS60404G.

[43] J.-W. Sun, P.-F. Yan, G.-H. An, J.-Q. Sha, G.-M. Li, G.-Y. Yang, Immobilization of polyoxometalate in the metal-organic framework rht-MOF-1: towards a highly effective heterogeneous catalyst and dye scavenger, Sci. Rep. 6 (2016) 25595, https://doi.org/10.1038/srep25595.

[44] J. Han, D. Wang, Y. Du, S. Xi, Z. Chen, S. Yin, T. Zhou, R. Xu, Polyoxometalate immobilized in MIL-101(Cr) as an efficient catalyst for water oxidation, Appl. Catal. A Gen. 521 (2016) 83–89, https://doi.org/10.1016/j.apcata.2015.10.015.

[45] H. Yang, J. Li, H. Zhang, Y. Lv, S. Gao, Facile synthesis of POM@MOF embedded in SBA-15 as a steady catalyst for the hydroxylation of benzene, Microporous Mesoporous Mater. 195 (2014) 87–91, https://doi.org/10.1016/j.micromeso.2014.04.023.

[46] P. Falcaro, R. Ricco, A. Yazdi, I. Imaz, S. Furukawa, D. Maspoch, R. Ameloot, J.D. Evans, C.J. Doonan, Application of metal and metal oxide nanoparticles@MOFs, Coord. Chem. Rev. 307 (2016) 237–254, https://doi.org/10.1016/j.ccr.2015.08.002.

[47] R. Fazaeli, H. Aliyan, M. Moghadam, M. Masoudinia, Nano-rod catalysts: building MOF bottles (MIL-101 family as heterogeneous single-site catalysts) around vanadium oxide ships, J. Mol. Catal. A Chem. 374–375 (2013) 46–52, https://doi.org/10.1016/j.molcata.2013.03.020.

[48] I. Boldog, P. Čičmanec, Y. Ganjkhanlou, R. Bulánek, Surfactant templated synthesis of porous VO x -ZrO 2 catalysts for ethanol conversion to acetaldehyde, Catal. Today 304 (2018) 64–71, https://doi.org/10.1016/j.cattod.2017.08.034.

[49] I.E. Wachs, B.M. Weckhuysen, Structure and reactivity of surface vanadium oxide species on oxide supports, Appl. Catal. A Gen. 157 (1997) 67–90, https://doi.org/10.1016/S0926-860X(97)00021-5.

[50] T.V. Andrushkevich, V.V. Kaichev, Y.A. Chesalov, A.A. Saraev, V.I. Buktiyarov, Selective oxidation of ethanol over vanadia-based catalysts: the influence of support material and reaction mechanism, Catal. Today 279 (2017) 95–106, https://doi.org/10.1016/j.cattod.2016.04.042.

[51] C.A. Carrero, R. Schloegl, I.E. Wachs, R. Schomaecker, Critical literature review of the kinetics for the oxidative dehydrogenation of propane over well-defined supported vanadium oxide catalysts, ACS Catal. 4 (2014) 3357–3380, https://doi.org/10.1021/cs5003417.

[52] B. Beck, M. Harth, N.G. Hamilton, C. Carrero, J.J. Uhlrich, A. Trunschke, S. Shaikhutdinov, H. Schubert, H.-J. Freund, R. Schlögl, J. Sauer, R. Schomäcker, Partial oxidation of ethanol on vanadia catalysts on supporting oxides with different redox properties compared to propane, J. Catal. 296 (2012) 120–131, https://doi.org/10.1016/j.jcat.2012.09.008.

[53] L.J. Lakshmi, Z. Ju, E.C. Alyea, Synthesis, characterization, and activity studies of vanadia supported on zirconia and phosphorus-modified zirconia, Langmuir 15 (1999) 3521–3528, https://doi.org/10.1021/la981103m.

[54] I.E. Wachs, Raman and IR studies of surface metal oxide species on oxide supports: supported metal oxide catalysts, Catal. Today 27 (1996) 437–455, https://doi.org/10.1016/0920-5861(95)00203-0.

[55] B. Kilos, A.T. Bell, E. Iglesia, Mechanism and site requirements for ethanol oxidation on vanadium oxide domains, J. Phys. Chem. C. 113 (2009) 2830–2836, https://doi.org/10.1021/jp8078056.

[56] P. Čičmanec, K. Raabová, J.M. Hidalgo, D. Kubička, R. Bulánek, Conversion of ethanol to acetaldehyde over VOX-SiO2 catalysts: the effects of support texture and vanadium speciation, React. Kinet. Mech. Catal. 121 (2017) 353–369, https://doi.org/10.1007/s11144-017-1169-z.

[57] Z. Li, A.W. Peters, A.E. Platero-Prats, J. Liu, C.-W. Kung, H. Noh, M.R. DeStefano, N.M. Schweitzer, K.W. Chapman, J.T. Hupp, O.K. Farha, Fine-tuning the activity of metal–organic framework-supported cobalt catalysts for the oxidative dehydrogenation of propane, J. Am. Chem. Soc. 139 (2017) 15251–15258, https://doi.org/10.1021/jacs.7b09365.

[58] H.G.T. Nguyen, N.M. Schweitzer, C.Y. Chang, T.L. Drake, M.C. So, P.C. Stair, O.K. Farha, J.T. Hupp, S.T. Nguyen, Vanadium-node-functionalized UiO-66: a thermally stable MOF-supported catalyst for the gas-phase oxidative dehydrogenation of cyclohexene, ACS Catal. 4 (2014) 2496–2500, https://doi.org/10.1021/cs5001448.

[59] C.-D. Wu, M. Zhao, Incorporation of molecular catalysts in metal-organic frameworks for highly efficient heterogeneous catalysis, Adv. Mater. 29 (2017) 1605446, , https://doi.org/10.1002/adma.201605446.

[60] A. Arya, P.K. Tripathy, D.K. Bose, Thermal decomposition of ammonium metavanadate in a fluidized bed reactor, Thermochim. Acta 244 (1994) 257–265, https://doi.org/10.1016/0040-6031(94)80225-4.

[61] S. Devautour-Vinot, G. Maurin, F. Henn, C. Serre, T. Devic, G. Férey, Estimation of the breathing energy of flexible MOFs by combining TGA and DSC techniques, Chem. Commun. (Camb.) 37 (2009) 2733, https://doi.org/10.1039/b822834e.

[62] T. Zhao, F. Jeremias, I. Boldog, B. Nguyen, S.K. Henninger, C. Janiak, High-yield, fluoride-free and large-scale synthesis of MIL-101(Cr), Dalton Trans. 44 (2015) 16791–16801, https://doi.org/10.1039/C5DT02625C.

[63] W.M.H. Sachtler, N.H.D. de Boer, North-Holland Publishing Company, Amsterdam, Proceedings, 3-rd International Congress on Catalysis (1964).
[64] P. Van Der Voort, K. Leus, Y.-Y. Liu, M. Vandichel, V. Van Speybroeck, M. Waroquier, S. Biswas, Vanadium metal–organic frameworks: structures and applications, New J. Chem. 38 (2014) 1853–1867, https://doi.org/10.1039/C3NJ01130E.
[65] B. Civalleri, F. Napoli, Y. Noël, C. Roetti, R. Dovesi, Ab-initio prediction of materials properties with CRYSTAL: MOF-5 as a case study, CrystEngComm 8 (2006) 364–371, https://doi.org/10.1039/B603150C.
[66] H. Leclerc, T. Devic, S. Devautour-Vinot, P. Bazin, N. Audebrand, G. Férey, M. Daturi, A. Vimont, G. Clet, Influence of the oxidation state of the metal center on the flexibility and adsorption properties of a porous metal organic framework: MIL-47(V), J. Phys. Chem. C. 115 (2011) 19828–19840, https://doi.org/10.1021/jp206655y.
[67] S. Biswas, D.E.P. Vanpoucke, T. Verstraelen, M. Vandichel, S. Couck, K. Leus, Y.-Y. Liu, M. Waroquier, V. Van Speybroeck, J.F.M. Denayer, P. Van Der Voort, New functionalized metal–organic frameworks MIL-47-X (X = −Cl, −Br, −CH3, −CF3, −OH, −OCH3) synthesis, characterization, and CO2 adsorption properties.pdf, J. Phys. Chem. C 117 (2013) 22784–22796, https://doi.org/10.1021/jp406835n.
[68] J.-C. Panitz, A. Wokaun, Effects of excitation wavelength on the Raman Spectra of vanadium(V) oxo compounds, J. Phys. Chem. 100 (1996) 18357–18362, https://doi.org/10.1021/jp961923c.
[69] L.J. Burcham, X. Gao, G. Deo, I.E. Wachs, In situ IR, Raman, and UV-Vis DRS spectroscopy of supported vanadium oxide catalysts during methanol oxidation, Top. Catal. 11/12 (2000) 85–100, https://doi.org/10.1023/A:1027275225668.
[70] H.M. Gobara, R.S. Mohamed, S.A. Hassan, F.H. Khalil, M.S. El-Sall, Pt and Ni nanoparticles anchored into metal–organic frameworks MIL-101 (Cr) as swift catalysts for ethanol dehydration, Catal. Lett. 146 (2016) 1875–1885, https://doi.org/10.1007/s10562-016-1826-2.
[71] P. Čičmanec, Y. Ganjkhanlou, J. Kotera, J.M. Hidalgo, Z. Tišler, R. Bulánek, The effect of vanadium content and speciation on the activity of VO_x/ZrO_2 catalysts in the conversion of ethanol to acetaldehyde, Appl. Catal. A Gen. (2018), https://doi.org/10.1016/j.apcata.2018.07.040.
[72] J.-H. Lee, S.J. Schmieg, S.H. Oh, Catalytic reforming of ethanol to acetaldehyde for Lean-NO x emission control, Ind. Eng. Chem. Res. 43 (2004) 6343–6348, https://doi.org/10.1021/ie049680v.
[73] M. Eckert, G. Fleischmann, R. Jira, H.M. Bolt, K. Golka, Acetaldehyde, Ullmann's Encycl. Ind. Chem. Wiley-VCH Verlag GmbH & Co., KGaA, Weinheim, Germany, 2006, https://doi.org/10.1002/14356007.a01_031.pub2.